A sonographic approach to prenatal classification of congenital spine anomalies

Debra Paoletti[1]
AMS MSci (Sonography)

Meiri Robertson[1]
MB, ChB, BSc MedSc (Hon)

Sock Bee Sia[2]
B App Sc (DR), M Ed, M Med (Sonography)

[1]Fetal Medicine Unit
Division of Women
Youth and Children
Canberra Hospital
Garran
Australian Capital Territory
Australia

Department of Obstetrics and Gynaecology
Australian National University
Acton
Australian Capital Territory
Australia

[2]Discipline of Medical Radiations
School of Medical Sciences
RMIT University
Melbourne
Victoria
Australia

Correspondence to email
debra.paoletti@act.gov.au

Abstract

Objective: To develop a classification system for congenital spine anomalies detected by prenatal ultrasound.

Methods: Data were collected from fetuses with spine abnormalities diagnosed in our institution over a five-year period between June 2005 and June 2010. The ultrasound images were analysed to determine which features were associated with different congenital spine anomalies. Findings of the prenatal ultrasound images were correlated with other prenatal imaging, post mortem findings, post mortem imaging, neonatal imaging, karyotype, and other genetic workup. Data from published case reports of prenatal diagnosis of rare congenital spine anomalies were analysed to provide a comprehensive work.

Results: During the study period, eighteen cases of spine abnormalities were diagnosed in 7819 women. The mean gestational age at diagnosis was 18.8w ± 2.2 SD. While most cases represented open NTD, a spectrum of vertebral abnormalities were diagnosed prenatally. These included hemivertebrae, block vertebrae, cleft or butterfly vertebrae, sacral agenesis, and a lipomeningocele. The most sensitive features for diagnosis of a spine abnormality included flaring of the vertebral arch ossification centres, abnormal spine curvature, and short spine length. While reported findings at the time of diagnosis were often conservative, retrospective analysis revealed good correlation with radiographic imaging. 3D imaging was found to be a valuable tool in many settings.

Conclusions: Analysis of the study findings showed prenatal ultrasound allowed detection of disruption to the normal appearances of the fetal spine. Using the three features of flaring of the vertebral arch ossification centres, abnormal spine curvature, and short spine length, an algorithm was devised to aid with the diagnosis of spine anomalies for those who perform and report prenatal ultrasound.

Keywords: prenatal sonography, prenatal ultrasound, vertebral defects.

Introduction

Prenatal ultrasound is a well established screening tool for fetal anomalies, and in Australia, this is performed at 18–20 weeks gestation. Advances in ultrasound technology have enabled visualisation of the fetus and fetal spine in more detail than ever before. Neural tube defects are the most frequent spine malformations and account for 4.6 cases per 10000 births in Australia.[1] These figures account mostly for open neural tube defects including anencephaly. The incidence of closed neural tube defects is uncertain, as is the incidence of vertebral abnormalities that do not involve the neural tube.

While open neural tube defects are associated with a poor prognosis,[2] the prognosis (and in particular, the long term prognosis) for other congenital spinal lesions can be difficult to determine. There is also an association between subtle spine lesions and certain multi-system syndromes.[3]

Classification systems for congenital spine anomalies exist, but these have been developed for the paediatric population. Works by Tortori-Donato, *et al.*[4], and others[5,6,7] are based on radiologic appearances. Other classifications are based on embryology and surgical experience.[8] Due to the rarity of these lesions, classification of congenital spine anomalies is complex, and terminology often confusing, as some authors have employed the same terminology to describe different entities. In addition, different lesions are often categorised together, leading to misleading prognostic conclusions. For those performing or reporting prenatal ultrasound, the issue is how to relate data derived radiologically or surgically in children to the ultrasound images of the fetal spine.

Recent advances in ultrasound technology have allowed examination of the fetus with improved resolution, and the advent of 3D ultrasound has allowed visualisation of the fetal spine in ways not previously possible. This has

enabled visualisation of a range of rare and subtle spine anomalies and led to diagnostic dilemmas, as existing classification systems do not relate readily to prenatal ultrasound.

The aim of this paper is to develop a comprehensive framework for congenital spine anomalies detected by prenatal ultrasound. The embryological basis for these defects will be described, as well as the process of mineralisation of vertebral elements in the fetus and normal sonographic features of the spine. This paper will begin by defining terminologies that appear in current literature in an effort to reduce confusion.

Terminology

Dysraphism is the term used to describe incomplete closure of the neural tube. This results in failure of the embryonic vertebral arches to fuse and a degree of disruption to overlying tissue. When the spinal defect extends to the skin so that nervous tissue is exposed it is referred to as an open spinal dysraphism. These lesions are also described as open neural tube defects, open spinabifida, and spina bifida aperta.[9] In this paper, the more familiar term open neural tube defect (open NTD) will be used.

Closed spinal dysraphisms are spinal defects where the skin posterior to the lesion remains intact; however in up to 50% of cases there are stigmata present in the skin overlying the affected vertebral segment (pigmentation, dimple or hairy nevus). These defects are also termed closed neural tube defects, closed spina bifida, and spina bifida occulta.[9] In this paper, the term closed neural tube defect will be used (closed NTD).

According to French, as cited by Tortori-Donati, *et al*.[5], the correct use of spina bifida is when referring to a defective fusion of posterior spinal bony elements.

Within the two subsets of open NTD and closed NTD, further classifications are possible. The term placode refers to a segment of the embryonic neural plate that did not undergo neurulation. Its presence and position is used by Tortori-Donati, *et al*. to classify NTDs, and is important for surgical management.[9]

Methods

This was a retrospective study, analysing cases in which spine abnormalities were diagnosed at our institution, which provides tertiary level obstetric ultrasound services to a wide geographic area. Cases of anencephaly and encephalocele (traditionally included as part of the spectrum of open neural tube defects) were excluded from this study, as this study's primary focus was spinal anomalies. It was not in the scope of this study to source and analyse prenatal ultrasounds of congenital spine anomalies diagnosed in children.

With approval from the ACT HREC (human research ethics committee), data were collected from fetuses with spine abnormalities diagnosed in our institution between June 2005 and June 2010. Ultrasound examinations were performed by experienced obstetric sonographers and sonologists using ATL HDI 5000 (Bothell, Washington, USA) with curved array 5–2 MHz from June 2005 – December 2005, and GE Voluson 730 Expert (GE Medical Systems, Milwaukee, WI, USA) with 3D curved array 4–8 MHz from December 2005 to June 2010. The ultrasound criteria for diagnosis of a spine abnormality included a disruption to the normal appearances of the ossification centres and abnormal contour of the spine. These features were present in at least one of the standard imaging planes for the fetal spine, namely a widening of the spinal canal in the coronal view, splaying of neural arch ossification centres in the transverse view, and absence of an ossification centre or abnormal spine contour in the sagittal view. 3D imaging was performed in cases which presented after December 2005. The presence of the cranial features of the Chiari II malformation were diagnostic of open NTD, but did not preclude careful and detailed examination of the fetal spine. Findings of the prenatal ultrasound images were correlated with other prenatal imaging, post mortem findings, post mortem imaging, neonatal imaging, karyotype, and other genetic workup.

A literature search was performed using PubMed, Web of Science and Google Scholar for reported cases of prenatal diagnosis of closed NTD and vertebral segmentation or formation defects. Key words included the various types of closed NTD outlined in the Tortori-Donati, *et al*.[5], classification system (Table 3), types of vertebral defects, 'prenatal diagnosis', 'ultrasound', and 'sonography'.

Results

During the study period, eighteen cases of spine abnormalities were diagnosed in 7819 women. The mean gestational age at diagnosis was 18.8w ± 2.2 SD. While most cases represented open NTD, a spectrum of vertebral abnormalities was diagnosed prenatally. Findings are shown in Table 1.

Open neural tube defects (10/18)

Ten cases were open neural tube defects with associated Chiari II malformation. Of these cases, eight were referred to our unit after the diagnosis was suspected at the second trimester screening ultrasound. In these cases, the cranial features of the Chiari II malformation instigated tertiary referral (although one referral incorrectly reported Dandy-Walker malformation). The remaining two cases were referred to our unit prior to 18w for other indications (selective fetal reduction in a triplet pregnancy, and management of maternal type II diabetes).

Closed neural tube defects (1/18)

There was one case (case 16) of an unexpected lumbosacral mass associated with a closed NTD, referred to our unit for invasive testing following an increased risk for T21 at first trimester screen.

Vertebral abnormalities (2/18)

Two cases (case 13 and 17) were referred because of abnormal spine curvature reported at the second trimester screening ultrasound.

Multiple abnormalities (4/18)

Two cases (case 11 and 12) were referred to our unit after abdominal wall defects detected during the first trimester screening ultrasound. Additional findings were sacral agenesis and arthrogryposis of upper and lower limbs in case 11, and scoliosis in case 12. Scoliosis and a single kidney were found in case 14, while case 18 was diagnosed with scoliosis, renal agenesis and a lower limb defect.

Table 1: Details of spine abnormalities diagnosed prenatally.

Case	MA	Indication	US findings	Other prenatal investigations	Outcome	Examination after TOP or Postnatal investigations
1	17 G1P0	Suspected open NTD	18w: thoracolumbar open NTD, Chiari II malformation & severe ventriculomegaly	none	TOP 18w	Open NTD confirmed by external examination
2	38 G3P0	Embryo reduction in triplet pregnancy	17w: lumbar spine open NTD &Chiari II malformation twin 1	none	Selective fetal reduction 17w	Not performed
3	28 G1P0	Suspected open NTD	19w: lumbar spine open NTD, Chiari II malformation & moderate ventriculomegaly	none	TOP 19w	Open NTD confirmed by external examination
4	23 G4P3	suspected open NTD	20w: lumbosacral open NTD, Chiari II malformation	none	TOP 20w	Open NTD confirmed by external examination
5	27 G2P1	suspected open NTD	21w: lumbosacral open NTD (myelomeningocele) &Chiari II malformation	none	TOP 21w	Open NTD confirmed by external examination
6	27 G2P1	suspected open NTD	21w: subtle defect sacral spine (open NTD) &Chiari II malformation	none	TOP 21w	Open NTD confirmed by external examination
7	22 G3P2	suspected open NTD	21w: lumbosacral open NTD (meningomyelocele) &Chiari II malformation	none	TOP 21w	Open NTD confirmed by external examination
8	39 G1P0	First trimester screening	12w: risk for T21 (1:4) and T13/18 (1:3) 17w: Sacral open NTD &Chiari II malformation, AVSD, bilateral talipes, growth restriction	Karyotype 47 XY + 18	Expectant management – FDIU 30w	Open NTD confirmed by external examination
9	38 G2P0	Suspected Dandy-Walker malformation	19w: open spina bifida &Chiari II malformation	none	TOP 20w	Open NTD confirmed by external examination
10	27 G1P0	suspected open NTD	20w: lumbosacral open NTD involving 6 segments &Chiari II malformation	none	TOP 21w	Open NTD confirmed by external examination
11	26 G3P2	gastroschisis	15w: gastroschisis 17w: Gastroschisis, upper & lower limb arthrogryposis, Sacral agenesis	none	TOP 17w	Post mortem examination: bilateral talipes, probable ruptured omphalocele, limb contractures with pterygia Post mortem radiology did not comment on sacrum Diagnosis: limb body wall complex
12	34 G1P0	Multiple structural abnormalities	14w: Exencephaly, spinal scoliosis, evisceration of abdominal and thoracic organs – features of Pentalogy of Cantrell	none	Surgical TOP 14w	Not possible
13	28 G1P0	scoliosis	21w: lower thoracic and lumbar hemivertebrae; fused ribs & extra rib on R; Possible sacral agenesis	Karyotype 46XX; Prenatal MRI at 22w non-diagnostic	TOP 23w	Post mortem radiology : abnormalities in all thoracic vertebrae (coronal clefts & butterfly vertebrae), sacral agenesis, 7 ribs on L, 9 ribs on R Post mortem examination: no dysmorphism, short trunk due to thoracic vertebral abnormalities, long arms, fused ribs, pulmonary hypoplasia Diagnosis: Most likely to be spondylocostal dysplasia Genetics: associated genes tested & showed no mutations in parents

14	28 G2P1	CVS - Increased risk on FTS	12w: abnormal spine curvature 16w: thoracic kyphosis, possible single pelvic kidney 18w: multiple hemivertebrae	46XX	TOP 19w	Post Mortem Examination: Vertebral irregularities with notochord remnant in the thoracic vertebrae, absent R kidney, hypoplastic uterus, anal opening abutting labial cleft, membraneous VSD, 5th finger clinodactyly, lung hypoplasia Post Mortem Radiology: Multiple hemivertebrae (T1-T8) with scoliosis to L, 11 ribs on R & 13 on L, 4 sacral segments Diagnosis: VATERR or MURCS
15	21 G2P0	Increased NF and small cerebellum	20w: Small cerebellum, multiple hemivertebrae& fused ribs	Declined	Live birth at 38w 2530g male	External examination: low set ears, flat philtrum, small jaw, prominent intra-orbital creases, finger & toe webbing, sacral dimple,wide spaced nipples & pectus excavatum, bilateral inguinal hernia Radiology: T6 hemivertebra, fused ribs & absent T12 rib MR: Small cerebellum & posterior fossa, syringohydromelia at cervicothoracic junction, conus terminates at L2/3 US: Normal kidneys Diagnosis: De novo 6p 27 deletion. Some features may also be due to exposure to sodium valproate
16	27 G2P1	Amniocentesis - Increased risk on FTS	18w: small lumbosacral mass, splayed lumbosacral vertebrae	Karyotype 46XX Normal amniotic AFP	TOP 21w	Post Mortem Examination: Partial sacral agenesis, lumbosacral mass containing fat and adherent meninges but no herniation of the spinal cord Post Mortem Radiology: partial sacral agenesis Diagnosis: Lipomenigocele with partial sacral agenesis
17	19 G1P1	scoliosis	21w: hemivertebrae at two levels 30w: no additional findings	Declined	Live birth at 39w 2915g female	Radiology: L unilateral segmentation defect at T10/11 & resultant R scoliosis, bilateral segmentation defect at L4/5 with resultant block vertebra & narrowing of spinal canal,11 ribs on L Other investigations declined
18	19 G1P0	Suboptimal imaging at FTS	20w: Oligohygramnios, renal agenesis, echogenic bowel, hemivertebrae & limb reduction defect of L lower leg	Karyotype 46 XY	TOP 21w	Post Mortem examination: Renal agenesis, trachea-oesophageal fistula, anorectal agenesis, absent distal tibia, fibula & foot of L lower limb Post Mortem radiology: Hypoplastic thumbs, hypoplastic R ilium, no evidence of hemivertebrae on radiographs taken Diagnosis: VACTERL

MA – maternal age, G – gravida, P – para, NTD – neural tube defect, FTS – first trimester screen, TOP – termination of pregnancy, AFP – alpha-fetoprotein, AVSD – atrio-ventricular septal defect, NF – nuchal fold, MRI – magnetic resonance imaging, FDIU – fetal death in utero

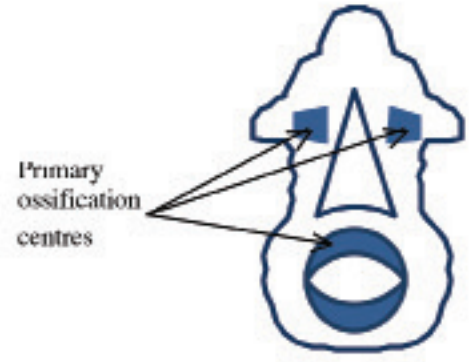

Figure 1: Diagrammatic representation of ossification centres found in each vertebra. Adapted from Kaplan, *et al.*[10]

Increased risk for T21 at combined first trimester screening (2/18)

Two cases (case 14 and 16) were referred for invasive testing following an increased risk for T21 after combined first trimester screening. Abnormal spine curvature was detected in case 14 at 12 weeks during the pre-procedure scan. Follow up at 16w and 18w demonstrated multiple hemivertebrae and a single kidney. Case 16 presented at 18w for invasive testing. A closed NTD associated with a lumbosacral mass was detected during the pre-procedure scan.

Other indications (2/18)

One case (case 18) was referred for a routine morphology scan as suboptimal imaging in the 11–14 week scan was reported. Findings included oligohydramnios due to renal agenesis, hemivertebrae, and a lower limb reduction defect.

Vertebral abnormalities (hemivertebrae and fused ribs) were additional findings in case 15, referred for review for a small cerebellum and increased nuchal fold.

Risk factors (3/18)

The majority of women presented with no known risk factors. One case (case 15) was associated with teratogenic maternal medication (valproate), and one (case 8) with maternal diabetes. In both cases the fetuses were also chromosomally abnormal, making the contribution of maternal risk factors difficult to ascertain. One case (case 7) involved consanguineous parents.

Outcomes

Termination of pregnancy occurred in fifteen of the eighteen cases; nine cases of open NTD (including selective fetal reduction in the multiple pregnancy), one case of closed NTD, four cases of multiple abnormalities, and one case of multiple vertebral abnormalities. One case of open NTD in a fetus with trisomy 18 was managed expectantly with subsequent spontaneous fetal demise at 30w. There were two live births at term. One baby was found to have dysmorphic features; karyotype revealed a chromosome deletion (6p27). The other baby had plain x-rays at day 1, confirming vertebral abnormalities but further follow up has been declined.

Discussion

Knowledge of the normal development of the spine and spinal cord is important for understanding the embryological basis for congenital spine abnormalities, as well as an understanding of common associations. For those involved with prenatal ultrasound, a sound knowledge of the process of mineralisation of vertebral elements in the fetus is important.

Embryology of the spine

The key stages involved with formation of the musculoskeletal and neural elements of the spine occurs from week two to six of embryonic development. These formative processes are gastrulation, primary neurulation, and secondary neurulation.[9] A complex series of events involving genes, signalling pathways and metabolic processes is required for proper formation of the spine and spinal cord.[10] Embryological explanations of normal and abnormal spinal development are still evolving.[9]

Spine ossification and sonographic appearance of the spine

During the sixth week when vertebral structures begin to fuse, signals from the notochord and neural tube induce chondrification. Histologically, the spine starts to mineralise during the 8th week of development as the notochord disintegrates. Ossification centres can be found in three main areas of the vertebrae – the centrum (vertebral body) and in each vertebral arch (Figure 1).

Appearance of the vertebral body ossification centre is initially in the lumbothoracic region and is followed by rapid cranial progression and slower caudal progression. Vertebral arch ossification centre begin at the first cervical vertebrae and continues caudally. By 9 weeks, ossification centres are present in the vertebral body from T2–L2, and in the vertebral arches from C1–L1.[13]

At birth each vertebra consists of three bony parts connected by cartilage. The bony halves of the vertebral arch usually fuse in the first 3–5 years, beginning in the lumbar spine and progressing cranially.[14]

The fetal spine demonstrates linear growth[15] with discs growing at a faster rate than vertebral bodies.[14]

The level of the conus medullaris changes with gestational age. The conus ascends from the 5th coccygeal vertebra at 11 weeks (13 weeks menstrual age) to L4 at 18 weeks (20 weeks menstrual age). The conus generally reaches the adult level (the lower border of L1) at term, although some reports suggest this may not happen until 1–2 months of age.[14,16]

Detection of the three vertebral ossification centres was described in 1988.[17] Studies by Budoricket, *et al.*[18] describe ultrasound evaluation of changes in vertebral arch ossification. This was found to be in a predictable pattern in a caudal direction, with an additional vertebral level being ossified every 2 to 3 weeks from L5. S2 is ossified by 22w. Pooh and Pooh[17] demonstrated the changing appearance of normal vertebral structure from 9–22 weeks gestation using transvaginal 3D ultrasound. At 9 and 11 weeks early vertebral structure is visible. At 13 weeks, vertebral bodies and early ossification of vertebral arches is present. At 15 weeks, the vertebral arches are present, but are completely apart; the distance is wider at the lumbosacral level then at the thoracic level. At 19 weeks there is still some separation of the vertebral arches distally. These gaps are almost closed by 22 weeks. A similar pattern in visualisation of the vertebral ossification centres is observed with transabdominal

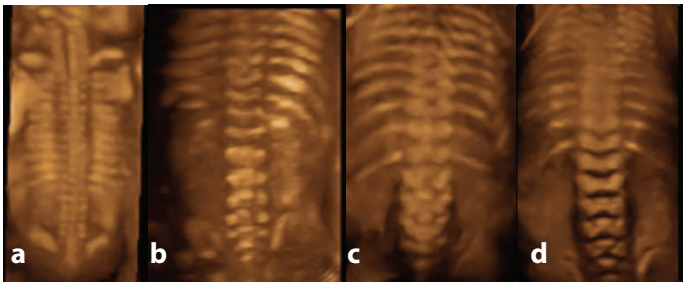

Figure 2: Appearance of normal fetal spine with 3D rendered transabdominal ultrasound at different gestations. A. 15 weeks – right and left vertebral arch ossification centres approach each other at the thoracic level but are still separate at the lumbosacral level. Note the absence of lumbosacral ossification at this gestation. B. 20 weeks – the three ossification centres in the lumbosacral region are readily apparent. C. 23 weeks & D. 25 weeks – vertebral arch ossification is complete.

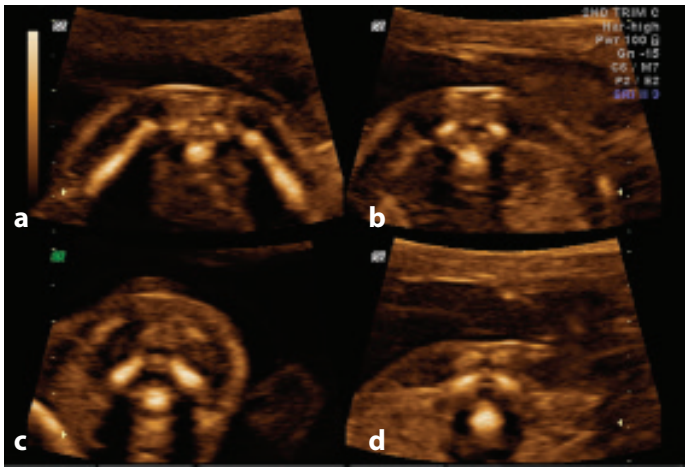

Figure 3: Transverse plane at 20 weeks. Note the subcutaneous tissue and intact skin line posterior to the vertebra at each level and the convergent orientation of the vertebral arch ossification centres. A. Sacral spine. Note the flattened triangular shape of the vertebra. B. Lumbar spine. Note the triangular shape of the vertebra. C. Cervical spine. Note the squarish shape of the vertebra. D. Thoracic spine. Note the triangular shape of the vertebra.

imaging (Figure 2), although with poorer resolution than what is possible with transvaginal imaging.

Sonographic assessment of the fetal spine is part of routine ultrasound screening for fetal abnormalities in the second trimester at 18–20 weeks. ISUOG guidelines,[13] describe the three planes that can be used to evaluate the integrity of the spine, often determined by fetal position. In the transverse plane, the spine is examined by moving the transducer along the entire length of the spine maintaining transverse orientation to each vertebra. Ossification centres of the body and vertebral arches are echogenic regions surrounding the neural canal. Lumbar and thoracic vertebrae are triangular in shape, sacral vertebrae are more flattened, and upper cervical vertebrae are more rectangular (Figure 3).

In the sagittal plane, ossification of the vertebral body and arches form two parallel lines that converge at the tip of the sacrum (Figure 4a). True mid-line sagittal can be achieved by angling through the unossified spinous processes to visualise the

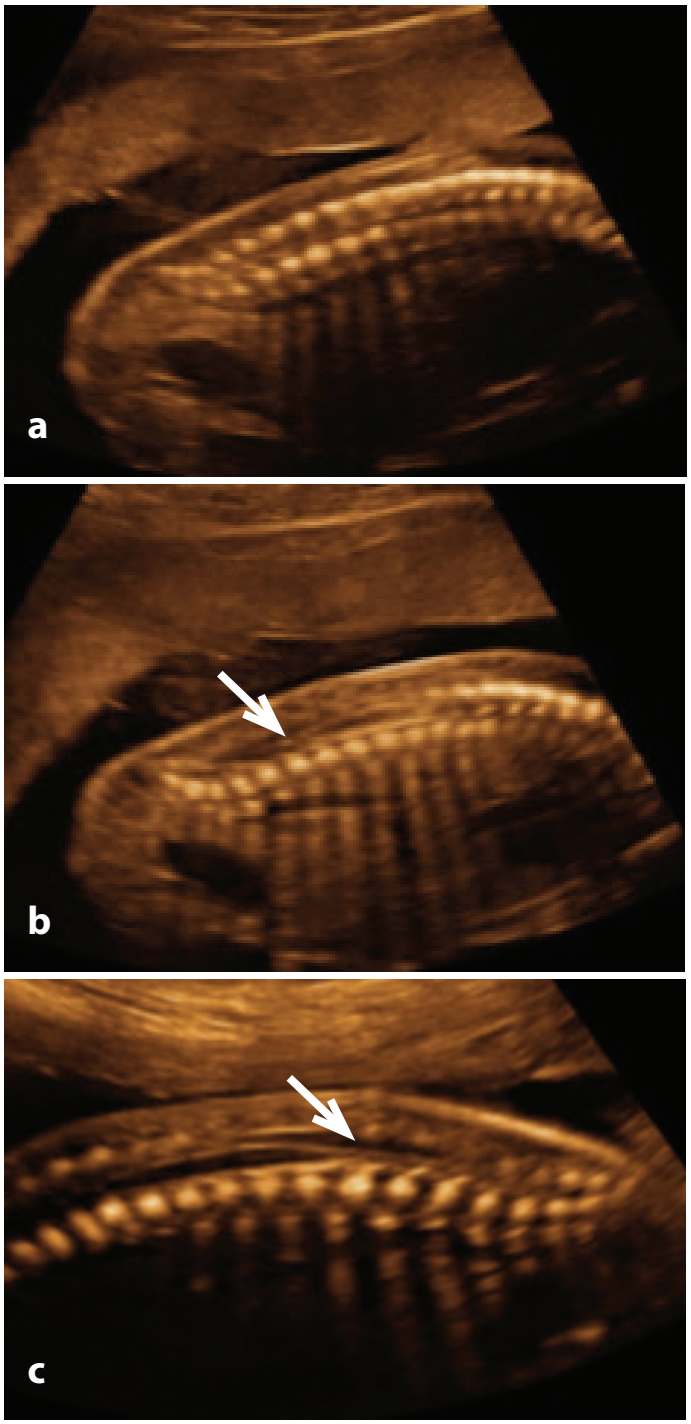

Figure 4: Sagittal plane at 20 weeks. A. Note the convergence of the ossification centres of the vertebral arch and body at the sacrum. B.& C. By angling the probe to image through the unossified spinous processes, the tip of the conus medullaris (arrow) can be visualised.

spinal canal and spinal cord (Figure 4b).

Coronally, it is possible to visualise all three ossification centres when orientated at the correct level, although in practice the vertebral arch ossification centres are typically visualised (Figure 5).

The advent of 3D ultrasound has made evaluation of the fetal spine more comprehensive. It allows for evaluation of the complete anatomy of the spine which is not always possible in 2D imaging due to the curvature of the spine.[19] Surface

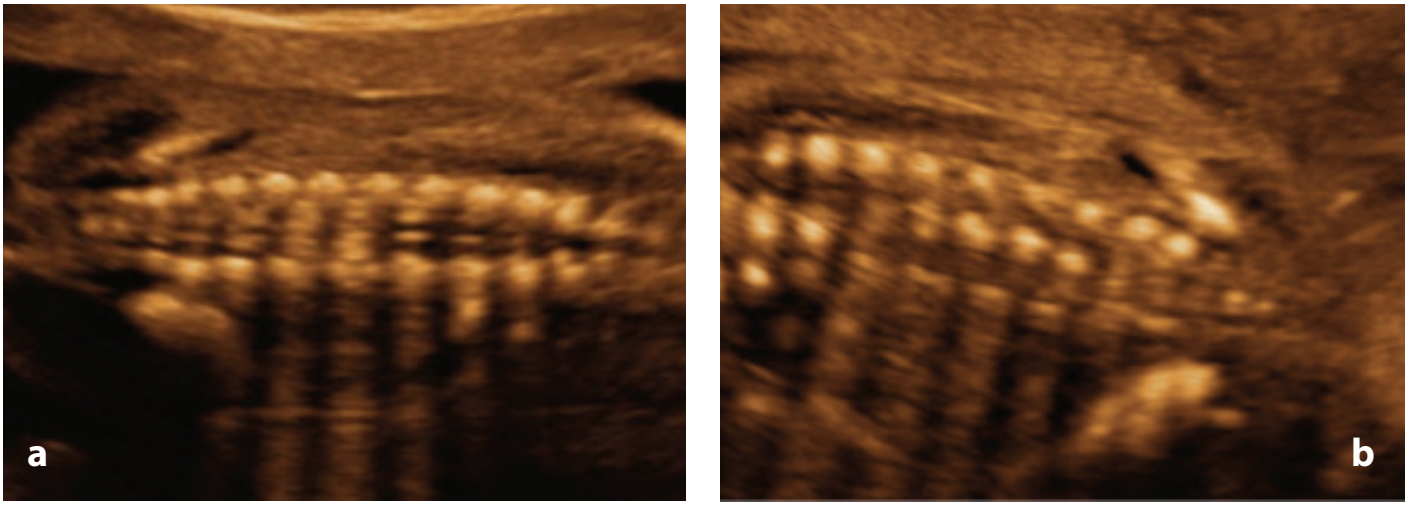

Figure 5: Coronal plane at 20 weeks. A. Note the distal convergence of the vertebral arch ossification centres. B. Note three ossification centres in the lumbosacral spine.

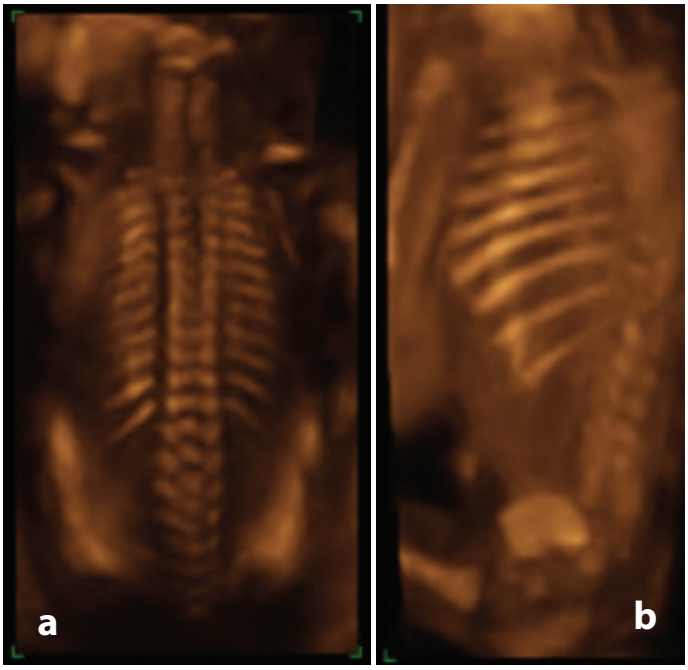

Figure 6: 3D rendered images of the spine at 20 weeks. A. Note the appearances of the vertebrae and the rib cage. B. By rotating the image, enhanced visualisation of the ribs is possible.

rendering functions allow the operator to enhance strong echoes from bone to allow evaluation of the complete fetal rib cage and scapulae (Figure 6).

Benoit[20] describes the use of multiplanar imaging where three planes of view and the rendered image may be viewed simultaneously. This allows for correct determination of the level of the conus medullaris (Figure 7).

Congenital spine defects

Embryologically, vertebral abnormalities can be classified as fusion defects, formation defects, and segmentation defects. Spinal cord abnormalities can be classified as errors of gastrulation, primary neurulation, or secondary neurulation.[9] Vertebral defects that usually do not involve the spinal cord are defects of formation and segmentation. Small fusion defects of the posterior vertebral arch may be isolated – these defects represent true spina bifida, and are believed to occur in 4% of the general population. The affected level is usually L5 or S1; laminae at this level may remain unfused in normal individuals until the age of 5–6 years.[9] As these lesions do not present for diagnosis prenatally, they will not be discussed further. When the spinal cord fails to fuse in neurulation, overlying vertebral elements also fail to fuse, resulting in large vertebral defects. A third group of defects arises from complex mechanisms. It is important to distinguish spinal cord versus vertebral (bony) abnormalities. The prognosis in general is much poorer in spinal cord abnormalities.

Developmental errors can occur at any stage of embryogenesis. Gastrulation is a highly sensitive stage of embryogenesis, and may be disrupted by genetic abnormalities and toxic insults.[11] Diabetic mothers have twice the background risk for congenital spine anomalies. Up to 30% of cases of sacral agenesis are associated with diabetic mothers.[7] Some drugs such as sodium valproate and folic acid antagonists also increase the risk.[24] Family history is an important consideration as syndromes, genetic disorders and chromosomal disorders are also associated with spinal defects. Anomalies of gastrulation involve errors of notochordal formation and integration. Spinal defects originating in this period are characteristically complex and involve other organs affected by notochordal development.[9] In primary neurulation, failure of the neural tube to close causes failure of the embryonic vertebral arches to fuse. Errors of secondary neurulation cause defects in the formation of the sacrum and filum terminale. The pathogenesis of some lesions is uncertain, and is the subject of debate.[7] Vertebral formation and segmentation defects occur due to errors in somite formation. Spine abnormalities may be a combination of all these mechanisms, resulting in complex structural abnormalities.[7,10]

Formation and segmentation defects

The prevalence of vertebral anomalies is 0.5–1 per 1000 live births[22] and may occur in one or multiple vertebrae.[23] The majority occur in the thoracic spine (64%), followed by the thoracolumbar spine (20%), lumbar spine (11%) and lumbosacral spine (5%).[22]

Abnormal vertebral development may result as a failure

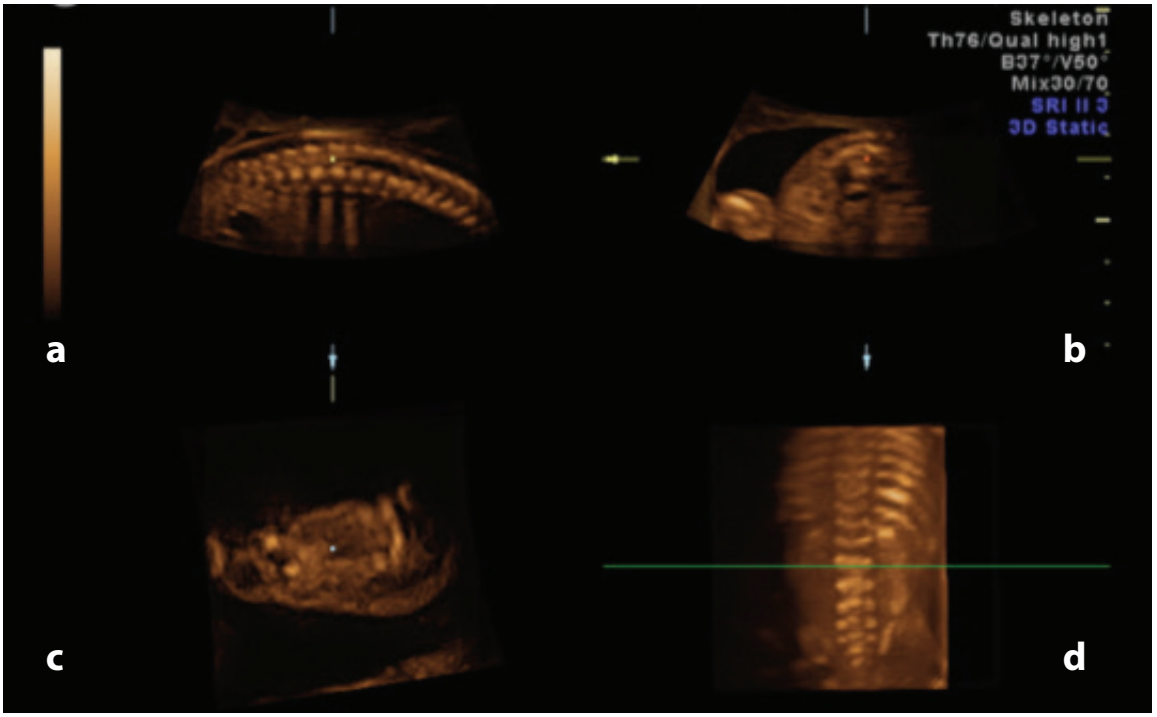

Figure 7: The use of multiplanar imaging to identify the level of the conus medullaris. A. Sagittal view. The dot is orientated at the tip of the conusmedullaris. B. Transverse view. When this is the reference image, a transverse line bisects the 3D rendered image (C) at the level of the dot. C. 3D rendered image. Visualisation of the spine and ribs allows for accurate counting of the vertebrae. In this case, the tip of the conus medullaris is at the level of the green line – L2.

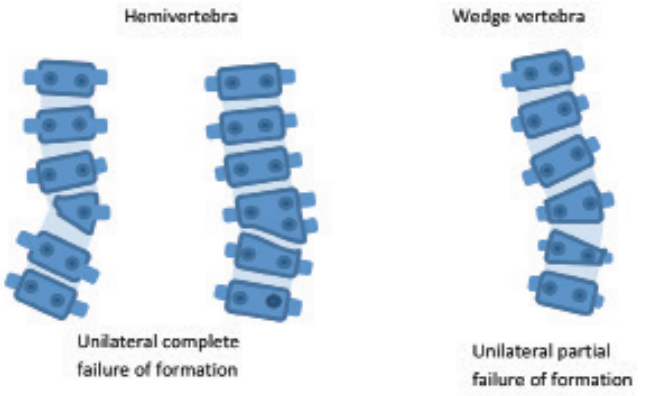

Figure 8: Schematic representation of formation defects. Adapted from Kaplan, *et al.*[10]

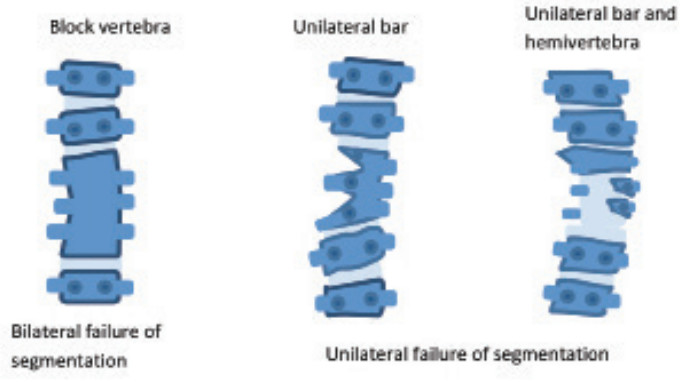

Figure 9: Schematic representation of segmentation defects. Adapted from Kaplan, *et al.*[10]

of formation, segmentation, or both, resulting in a congenital scoliosis.[10,22] Defects in formation occur when a structural element of a vertebra is absent, that is, there is a failure of an ossification centre to develop. Any region of the vertebral ring may be affected, and the resulting abnormality will depend on which area is affected.[10] Observable defects include hemivertebrae and wedge vertebrae (Figure 8).

When two adjacent somites do not separate properly, a segmentation defect will occur. The effects are variable and relate to which part and how much of the vertebra is involved. When entire vertebrae are involved, the result is block vertebrae.[10] Defects of specific regions of the vertebral ring create unilateral bars (Figure 9). Butterfly vertebrae result from a failure of fusion of the two lateral chondrification centres of a vertebral body due to the persistent presence of the notochord. The affected vertebra has a 'butterfly' shape.[7]

Although vertebral anomalies may be isolated, they are frequently associated with other anomalies, in particular renal anomalies (20–40%) and cardiac (10–15%).[21] There is an extensive list of syndromes and associations listed in Appendix 1.[24] Features of the more common syndromes associated with vertebral abnormalities are summarised in Table 2.[24]

The term association is used to describe the non-random tendency of some malformations to occur together more commonly than would be expected by chance. These include the acronyms VATERR, VACTERL and MURCS.[24] VATERR describes the association between vertebral defects, anal atresia, tracheo-oesophageal fistula, oesophageal atresia, radial dysplasia and renal dysplasia. VACTERL adds cardiac malformation and replaces radial dysplasia with limb abnormality. Another association is MURCS, which describes the association between Mullerian duct aplasia, renal aplasia and cervico-thoracic somite dysplasia.

There were six cases of vertebral abnormalities in this study.

Table 2: Syndromes associated with vertebral defects.
From *Smith's Recognisable Patterns of Human Malformation*[24]

Syndromes	Features
Goldenhar (oculo-auriculo-vertebral spectrum)	Incidence 1:3000–1:5000 Asymmetric unilateral hemifacialmicrosomia, hemivertebrae or hypoplastic vertebrae usually cervical but occasionally thoracic or lumbar
Klippel-Feil syndrome	Incidence 1:42000, autosomal dominant but usually sporadic Characterised by fused cervical vertebrae, sometimes associated with hemivertebrae, webbed neck & facial asymmetry. Congenital heart defects, renal abnormalities, rib abnormalities, Sprengel anomaly, cleft palate are other associations. Mental deficiency, primary or secondary neurologic deficits may occur.
Alagille syndrome (arteriohepatic dysplasia)	Incidence , autosomal dominant, variable expression Features include growth restriction, deep set eyes, abnormal ears, right heart or pulmonary circulation defects, hemivertebrae, abnormal ribs, paucity of intrahepatic bile ducts and chronic cholestasis.
Jarcho-Levin syndrome	Rare abnormality, autosomal recessive Characterised by 'crab-like' rib cage, multiple hemivertebrae, abnormal ribs and short trunk. Other features include cleft palate, triangular shaped mouth, imperforate anus, cardiac dextroposition, ASD, undescended testes, hydrocephalus (aqueduct stenosis), and neural tube defects. Resulting structural abnormalities of the chest means that affected individuals die of respiratory insufficiency or infection.
Spondylothoracicdysostosis (often grouped with Jarcho-Levin syndrome)	Rare abnormality, Autosomal recessive, variable expression Multiple vertebral segmentation defects are present, but the 'crab-like' features of Jarcho-levin syndrome are not present.
Spondylocistaldysostosis (often grouped with Jarcho-Levin syndrome)	Rare abnormality, Autosomal dominant Multiple vertebral segmentation defects throughout entire spine are present, which tend to be milder than those in Jarcho-Levin syndrome &Spondylothoracicdysostosis
Gorlin syndrome (nevoid basal cell carcinoma syndrome)	Incidence 1:60000, autosomal dominant Characterised by basal cell nevi (with carcinomatous potential) over face and upper body, macrocephaly, short metacarpals, abnormal ribs, cervical & thoracic vertebral abnormalities. Other features such as ectopic calcification of the falx cerebri, mental deficiency and agenesis of the corpus callosum have been reported.

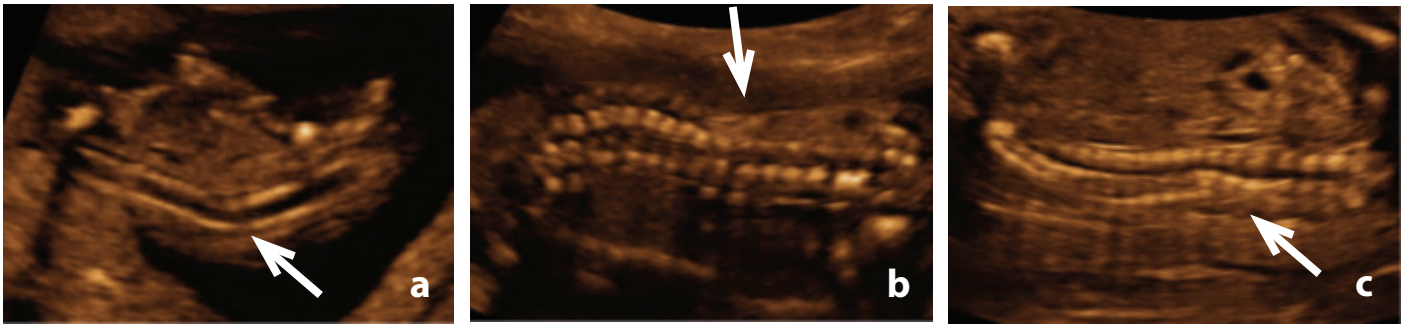

Figure 10: Abnormal spine curvature. A . Case 14 – abnormal spine curvature demonstrated at an early gestation (12 weeks) (arrow) B. Case 13 – abnormal curvature at 21 weeks (arrow) C. Case 18 – abnormal curvature at 20 weeks detected despite oligohydramnios (arrow).

In five cases cases 12, 13, 14, 17 & 18, the abnormal curvature of the spine in the sagittal plane led to the diagnosis of a vertebral abnormality (Figure 10a, b, c).

Clarification of the nature of the vertebral defect was often not possible in transverse and coronal planes due to suboptimal imaging conditions such as fetal lie and oligohydramnios. In this study, 3D imaging was found to be an extremely valuable tool, confirming findings by Benoit[20] and Moser.[23] Retrospective analysis of 3D images in case 13 demonstrated cleft or butterfly thoracic vertebrae and rib irregularities, namely asymmetrically reduced number and rib fusion (Figure 11). Review of 3D images revealed block vertebrae in case 17 (Figure 12) and hemivertebrae. Hemivertebrae were also discerned in case 15 (Figure 13).

Prognosis for congenital scoliosis relates to the presence and severity of associated abnormalities. Isolated hemivertebrae with scoliosis may progress slowly (50%), remain stable (25%) or progress rapidly (25%). Early surgical intervention is necessary in about 75% of cases to prevent curvature progression.[22,23]

Fusion defects

Failure of the neural tube to completely close in week 4 results in failure of the embryonic vertebral arches to fuse. When the defect involves the skin, an open NTD is the result. When the

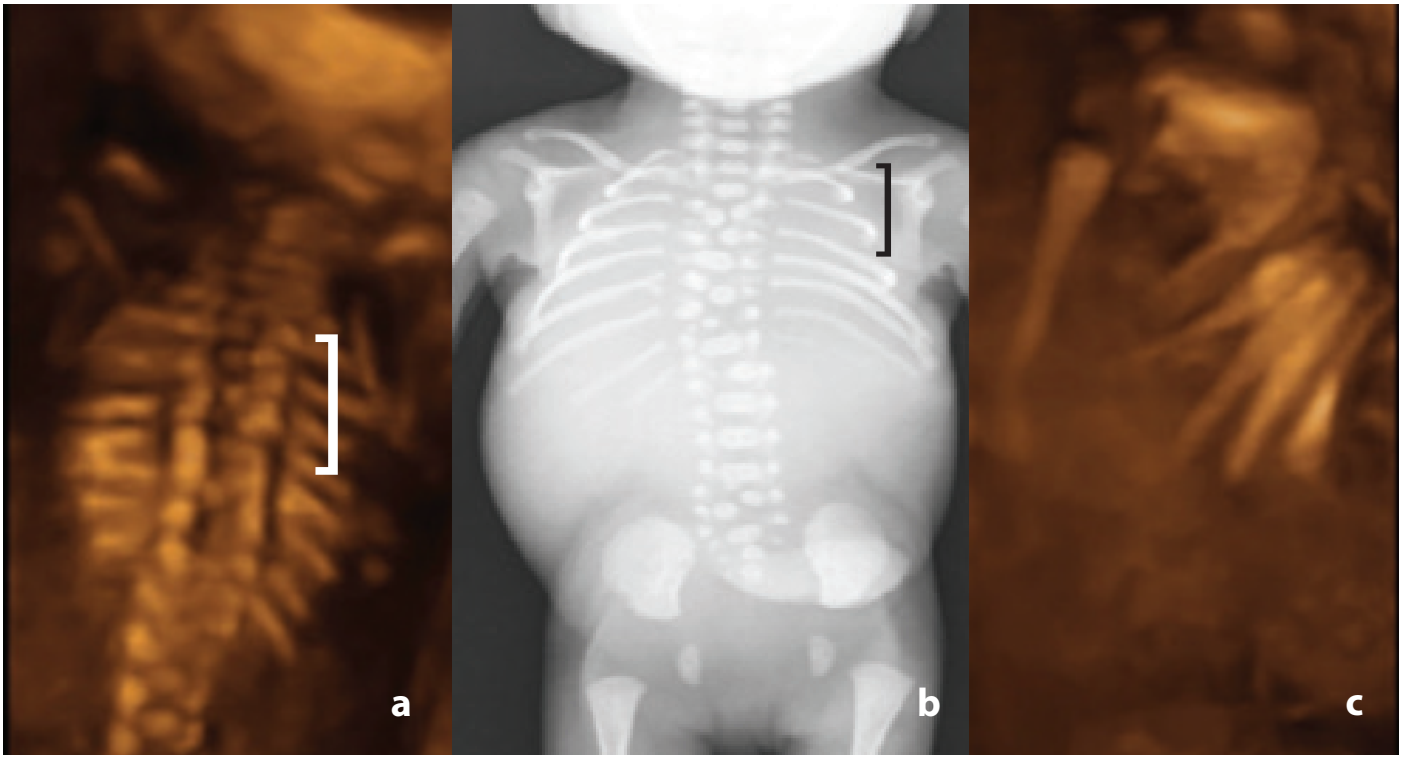

Figure 11: Cleft thoracic vertebrae – case 13. A. 3D coronal image acquired at 21 weeks gestation demonstrating cleft thoracic vertebrae (brace). Note the rib asymmetry (7 ribs on the right, 9 ribs on the left). B. Corresponding post mortem radiograph demonstrating thoracic butterfly vertebrae (brace) C. Rotating the 3D coronal dataset demonstrates rib fusion.

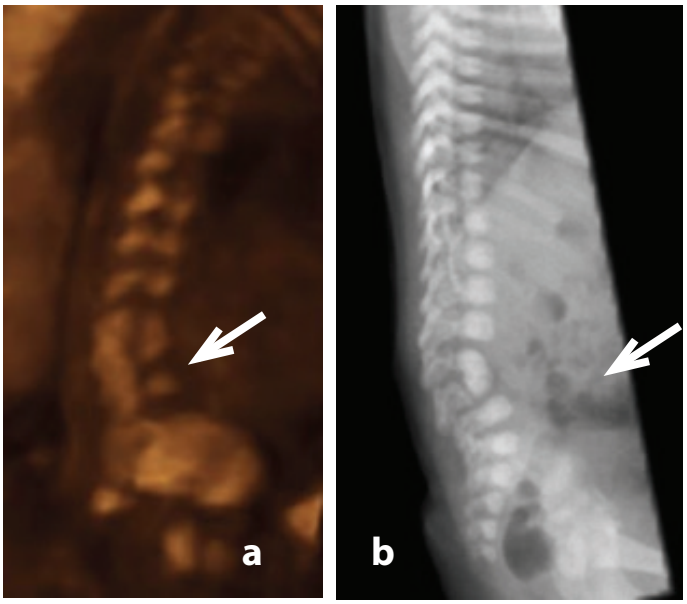

Figure 12: Block vertebrae – case 17. A. L4/5 block vertebrae revealed by rotating the 3D dataset acquired at 21 weeks gestation (arrow). B. Corresponding post natal radiograph.

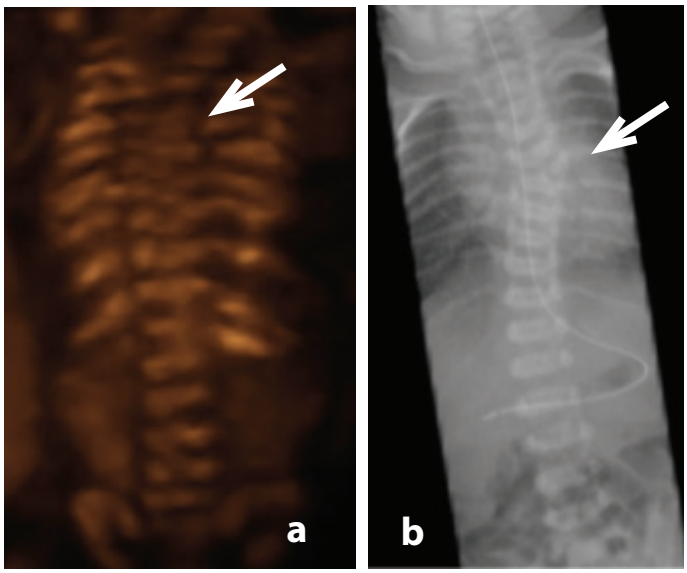

Figure 13: Hemivertebra – case 15. A. 3D coronal image demonstrating T6 hemivertebra at 19 weeks gestation (arrow).B. Corresponding post natal radiograph.

skin remains intact, these defects are referred to as closed NTD.[21]

Myelomeningoceles account for nearly 99% of open NTD.[9] Rarer presentations include myelocele, hemimyelocele and hemimyelomeningocele. Classification of these lesions is determined by the position of the placode (cells of the embryonic neural plate that did not undergo neurulation). The placode can be identified at post mortem, during surgery, or with MRI.[25] The placode is not a feature that can be discerned by prenatal ultrasound. In myelomeningoceles, the placode protrudes above the skin surface. In myeloceles, the placode remains flush with the skin surface. Hemimyelocele and hemimyelomeningocele are the extremely rare cases of myelocele and myelomeningocele associated with diastematomyelia (split cord malformation).[9]

Diagnosis of open NTD prenatally is well established,

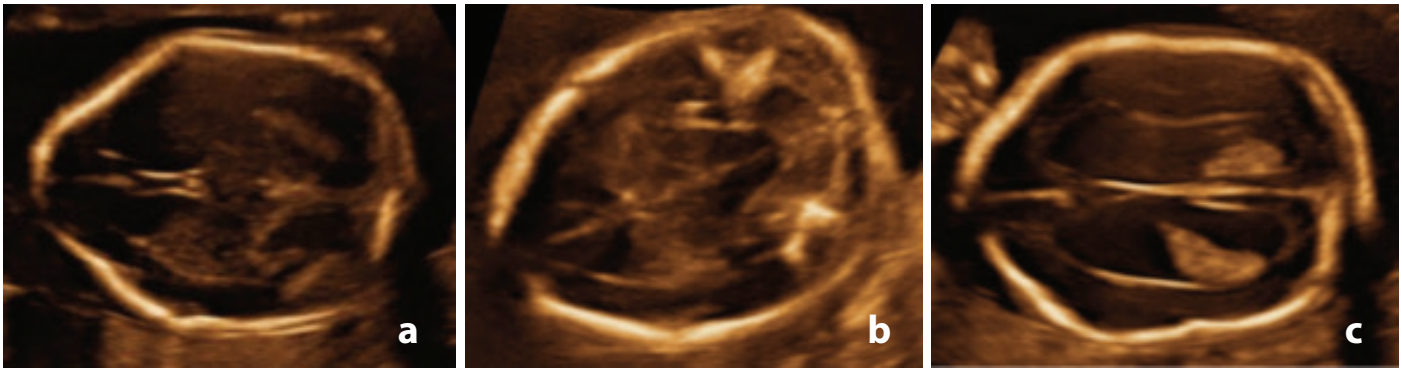

Figure 14: Cranial features of the Chiari II malformation in case 10. A. Frontal bossing or 'lemon' shaped head. B. Cerebellar distortion or 'banana' shaped cerebellum and obliterated cisterna magna. C. Marked ventriculomegaly.

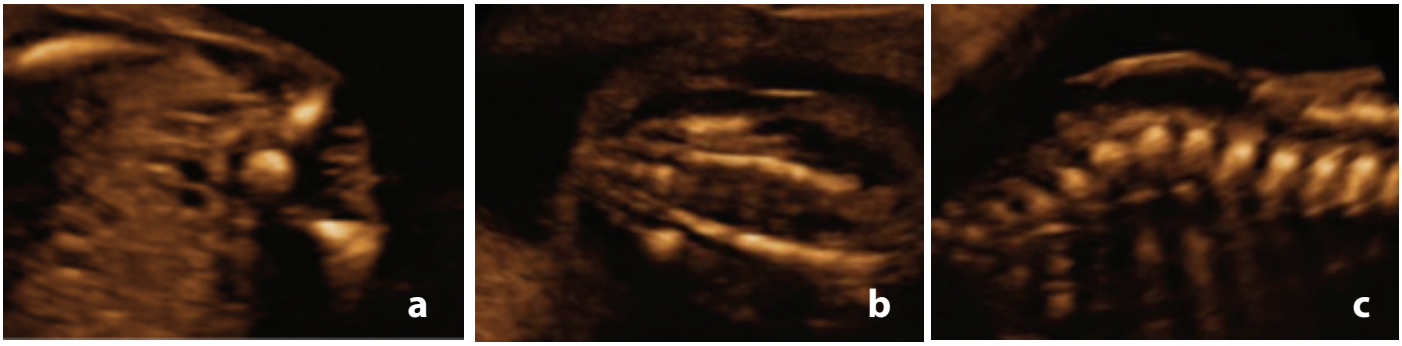

Figure 15: Vertebral features of open NTD – case 10. A. Flared vertebral arch ossification centres in transverse. Note the disruption to the subcutaneous tissue and skin line posterior to the vertebra. B. Widened vertebral arches in coronal. C. Disruption of the skin line posterior to the vertebral defect with bulging meninges.

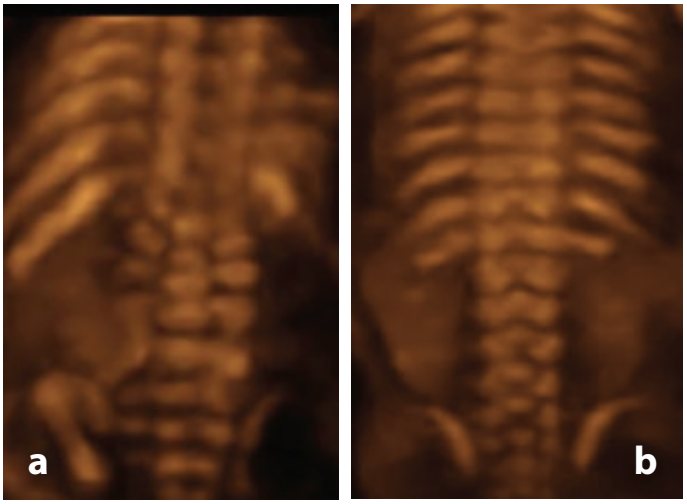

Figure 16: 3D rendered image of open NTD. A. Case 7 – widened lumbosacral spine indicative of a defect involving L2 to S5. B. Normal spine for comparison.

primarily due to the cranial features of the Chiari II malformation (Figure 14). The presence of the Chiari II malformation on prenatal ultrasound is diagnostic of open NTD. Nicolaides, *et al.*[26] described the sonographic features of the 'lemon' shaped head, 'banana' shaped cerebellum, obliterated cisterna magna and varying degrees of hydrocephalus. Identification of these striking features instigates careful examination of the spine to identify the spinal defect. According to Litiania and Passamonti,[27] it is believed prenatal ultrasound in second and third level centres is close to 100% accurate in the diagnosis of open spinal dysraphism.

This was reflected by the cases of open NTD in this study where the Chiari II malformation was present in all cases. Vertebral features were typically a disruption to the orientation of the ossification centres of the vertebra; namely flaring in transverse section (Figure 15a) and widening in coronal section (Figure 15b). Skin disruption behind the spine defect was evident in transverse or sagittal section (Figure 15a, 15c). 3D imaging was able to provide additional information by elegantly demonstrating the number of affected vertebral elements (Figure 16a).

Infant mortality varies considerably worldwide; almost 100% in underdeveloped countries and 10%-35% in developed countries. Survival to the third decade has been reported at 52–68%.[2] Surviving infants are likely to have severe life-long disabilities. Medical problems resulting from the neurologic defect or its repair include paralysis, hydrocephalus, endocrine abnormalities and tethered cord syndrome. Limb and spine deformation; bladder, bowel and sexual dysfunction; and learning disabilities frequently occur as a consequence.[2] Many parents choose to interrupt the pregnancy, as was the case in this study.

Closed NTD have been classified by Tortori-Rossi, *et al.*[5] as lesions presenting with a subcutaneous mass, and those without a subcutaneous mass. On the whole, this subclassification provides features that relate to detection with prenatal ultrasound. Definitions of these classifications along with embryonic classification[9] are summarised in Table 3, highlighting the fact that lesions which appear similar may have a different embryological basis.

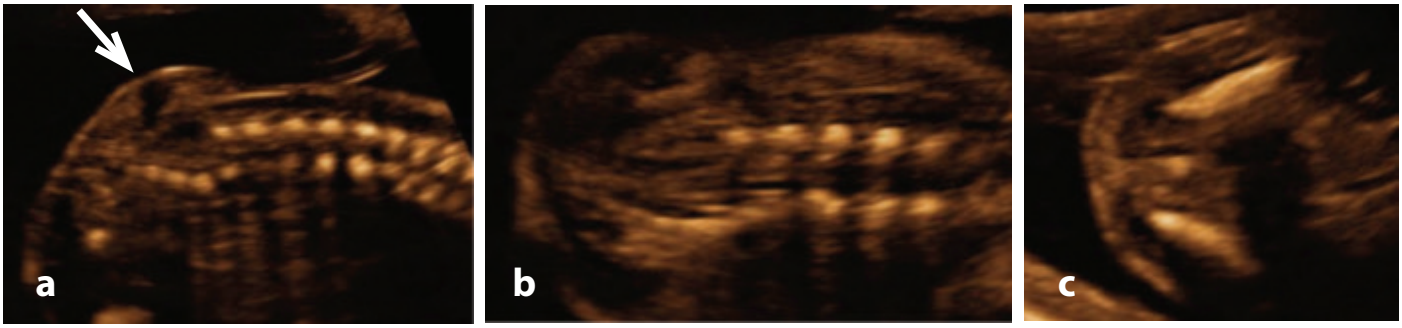

Figure 17: Lipomengocele – case 16. A. Sagittal view demonstrates a mostly echogenic subcutaneous mass with a central anechoic area (arrow). Note the absence of vertebral arch ossification centres. B. Coronal view demonstrating a widening of the lower spine and an absence of the vertebral arch ossification centres. C. Transverse view demonstrating a single ossification centre.

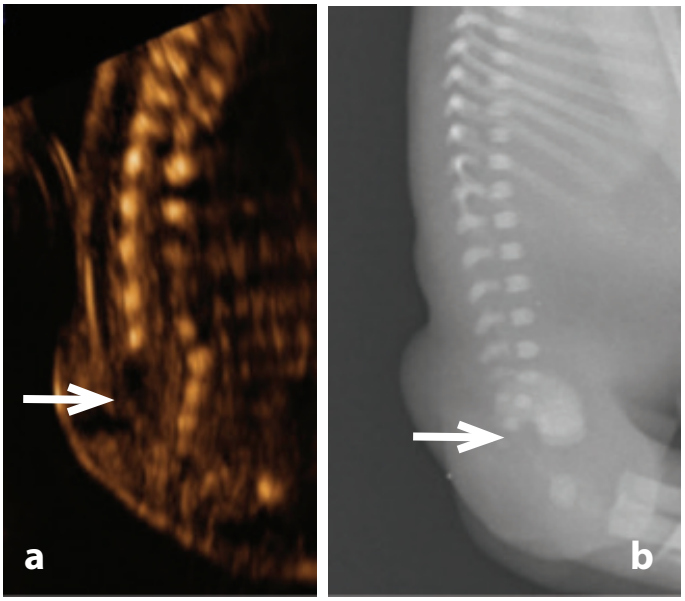

Figure 18: Lipomeningocele – case 16. A. Sagittal view demonstrating absent lower sacral elements (arrow) B. Post mortem radiology confirming partial sacral agenesis.

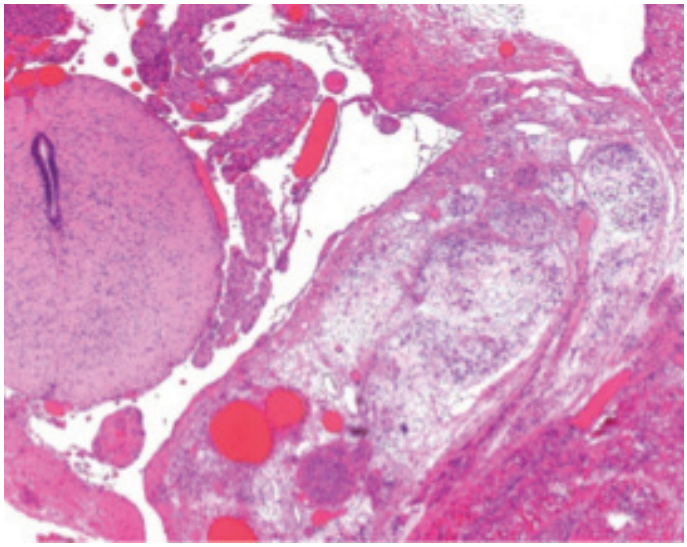

Figure 19: Histology of lipomeningocele. Histology from the mass demonstrating adipose tissue and meninges with adjacent normal appearing spinal cord.

Table 3: Summary of features of closed NTD.
Developed from Tortori-Donati, *et al.*[9]

With a subcutaneous mass		**Embryologic classification**	**Without a subcutaneous mass**		**Embryologic classification**
Lipomyelocele	Placode-lipoma interface within the spinal canal	Error of primary neurulation	Intradural lipoma	Lipoma within the dural sac	Error of primary neurulation
Lipmyelomeningocele	Placode-lipoma interface outside the spinal canal	Error of primary neurulation	Filar lipoma	Fibrolipomatous thickening of filum	Error of secondary neurulation
Lipomeningocele	Dorsal lipoma adherent to dura	Error of primary neurulation	Tight flium terminale	Hypertrophy and shortening of filum	Error of secondary neurulation
Meningocele	Herniation of CSF filled sac lined by dura	Error of unkown origin	Persistent terminal ventricle	Persistent cavity with conusmedullaris	Error of secondary neurulation
Terminal Myelocystocele	Terminal syrinx herniating into a posterior meningocele	Error of secondary neurulation	Dermal sinus	Epithelial lined fistula between neural tissue and skin surface	Error of gastrulation (notochordal integration)
Myelocystocele	Dilated central canal herniating through posterior vertebral defect	Error of primary neurulation			

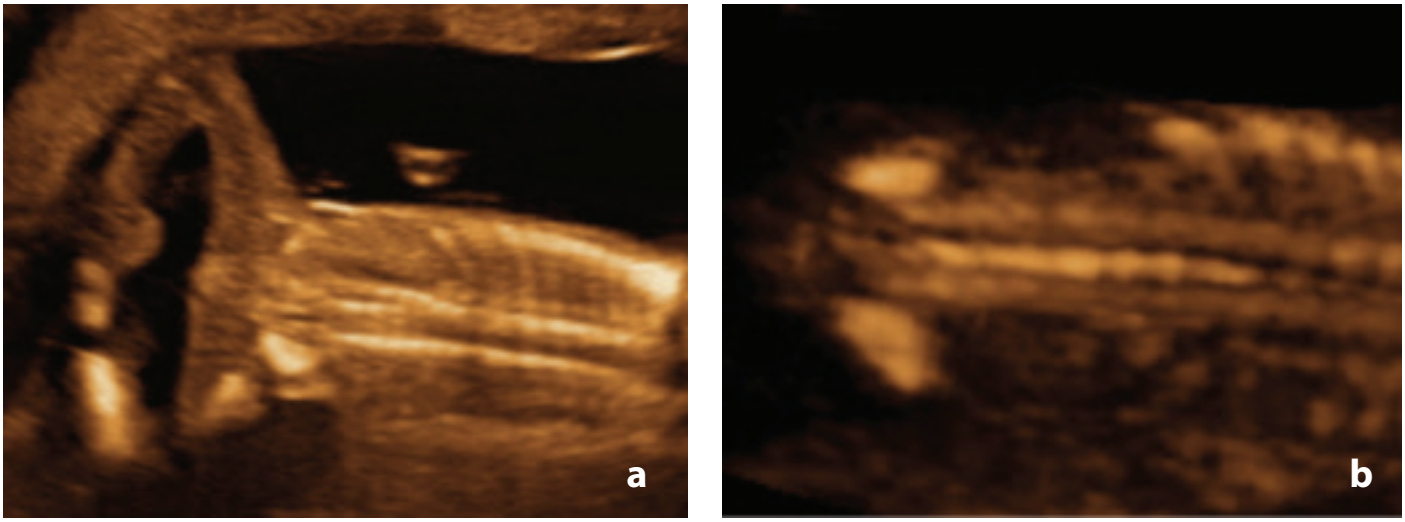

Figure 20: Sacral agenesis – Case 11 A. Coronal view at 15 weeks demonstrating an abrupt termination of the distal spine and lack of tapering of ossification centres toward each other. Note the lower limb arthrogryposis. B. Coronal view of a normal fetal spine at 15 weeks. Although sacral ossification is incomplete at this gestation, note the tapering of the distal spine.

Closed NTD with a subcutaneous mass represent nearly 19% of all closed NTD. Within this group, lipomyelomeningoceles are the most common.[9]

One case of a closed NTD was diagnosed in the study group (case 16). The presence of a lumbosacral mass was an important feature in this diagnosis. The sonographic features of the mass were mixed echogenicity (mid-level echoes with an anechoic central portion) and no discernable vascularity (Figure 17a). Widening of the lumbosacral spine in coronal section (Figure 17b) and flaring of the ossification centres in transverse section (Figure 17c) was indicative of a vertebral defect. Ossification centres of the lower sacral elements were not detected, leading to the diagnosis of partial sacral agenesis (Figure 18a). Differential diagnosis included sacrococcygeal teratoma and lipomyelomeningocele. The presence of sacral defects and echo characteristics of the mass were more typical of a lipomyelomeningocele; up to 50% of teratomas contain calcification.[7] Detection of an anechoic cystic structure within an echogenic mass is considered a diagnostic feature of a lipomyelomeningocele.[6] Post mortem examination and post mortem radiology confirmed the partial sacral agenesis (Figure 18b), however histology revealed the mass to be a lipomeningocele – the mass contained fat with herniated but not adherent meninges. No component of spinal cord was within the mass (Figure 19).

There were no cases in this study of a closed NTD without a subcutaneous mass. This group of lesions includes cord lipomas (intradural, intramedullary and filarlipomas), and tight filum terminale (where the filum terminale is thickened), persistent terminal ventricle and dermal sinus.[7,12]

Cord lipomas, typically lumbosacral in location, and tight filum terminale are associated with tethered cord syndrome. Prenatal detection has been reported.[28] Features which may be apparent on prenatal ultrasound include increased echogenicity and widening of the spinal cord due to the presence of a mass. The conus medullaris may be at a lower position than normal for gestational age.[27]

Detection of a terminal ventricle by prenatal ultrasound in the third trimester has been described as a cystic mass at the distal portion of a widened spinal canal.[29] However, it may be difficult to detect such lesions at earlier gestations, particularly if they are small. There have been no case reports of prenatal sonographic detection of a spinal dermal sinus. It is doubtful whether it would be possible to resolve the tiny skin defect associated with a dermal sinus at the time of routine prenatal ultrasound screening (18–20 weeks).

Prognosis for some of these lesions is often related to the presence and severity of other anomalies. Tethered cord syndrome, where nerve fibres are stretched and distorted, is seen in the presentation of some closed NTD, including lipomyelomeningocele, intradural lipoma and filar lipoma. Symptoms tend to be progressive in nature and include pain, sphincter disturbances, sexual dysfunction, distal paralysis and sensory deficits. Neurological deficits have been reported in up to 80% of patients with closed NTD.[3] Signs and symptoms may be present at birth, or may develop later in life. The position of the conus medullaris can be an important feature when making a prognosis based on prenatal findings. Visualisation of fetal leg movement and bladder emptying does not guarantee a good prognosis, however, evidence of limb contractures is indicative of a poor prognosis.[26]

Complex defects

Some conditions have been described as complex dysraphic states, believed to be due to either defective gastrulation and notochord development, or errors in secondary neurulation.[9] Tortori-Donati, *et al.*[5] lists complex defects as a subclassification of closed NTD without a mass.

In diastematomyelia there may be duplication of all or a portion of the spinal cord, accounting for about 4% of closed NTD.[9] Exceedingly rare conditions exist where there is a communication between spinal cord, bowel and even the skin surface (neurenteric cyst and dorsal enteric fistula). Hypogenesis or agenesis of a portion of the spine may occur; usually (but not always) distally. Sacral agenesis describes the condition when the distal portion of the spine and sacrum is absent, and is often referred to as caudal agenesis or caudal regression. Observable

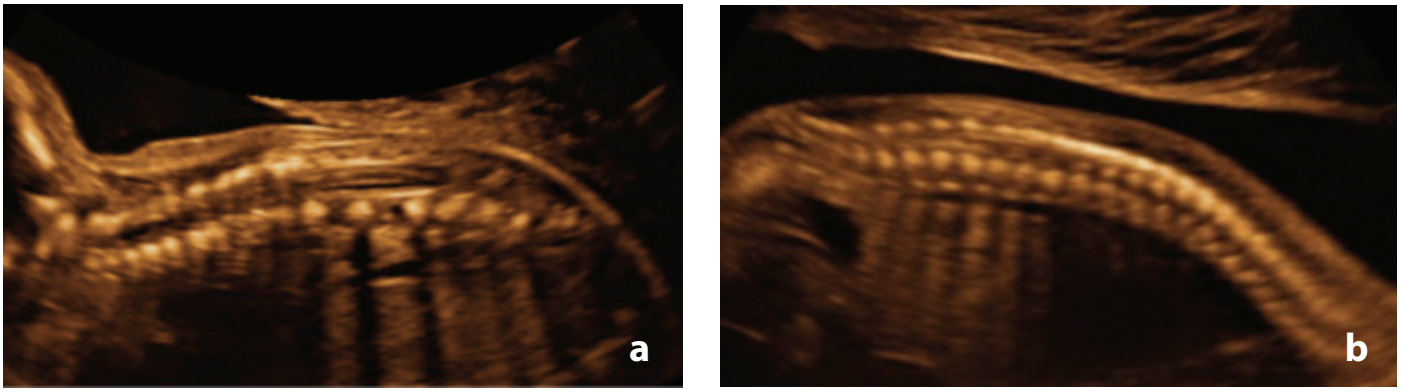

Figure 21: Sacral agenesis – Case 13 A. Sagittal view at 21 weeks demonstrating a shortened spine B. Sagittal view of a normal fetal spine at 21 weeks.

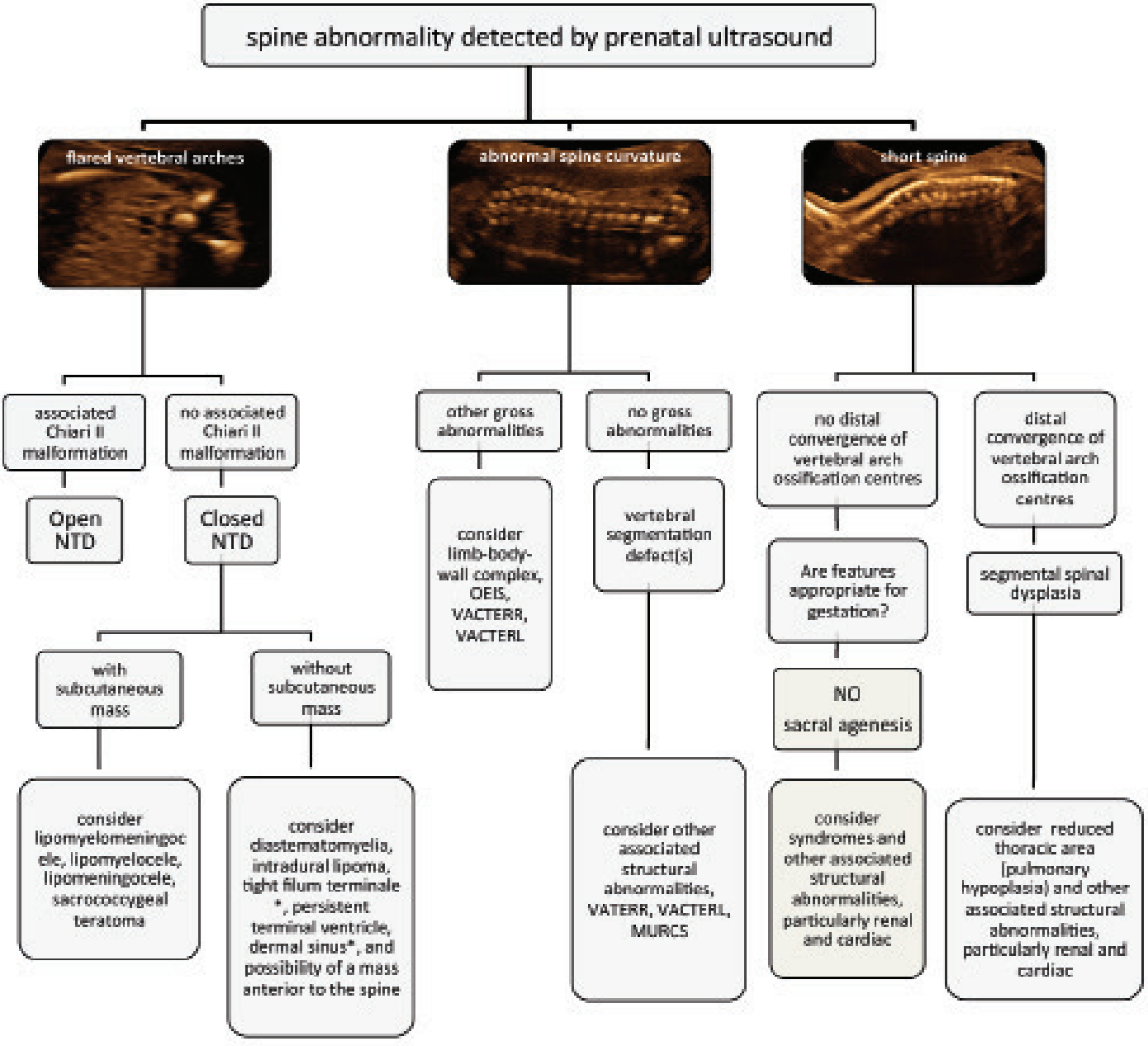

Figure 22: Algorithm based on sonographic features to aid in identification of congenital spine anomalies.

effects range from partial sacral agenesis to complete absence of the lower portion of the spinal column with associated abnormalities including renal dysplasia or agenesis, duodenal atresia, and tracheo-oesophageal atresia. Sirenomelia thought to be the most extreme expression of sacral agenesis. There are also reported associations, including VACTERL, OEIS (omphalocele, cloacal extrophy, imperforate anus, spinal deformity) and Currarino Syndrome (autosomal dominant condition characterised by partial sacral agenesis, anorectal malformation, and a presacral mass)[7,9,27]. Partial sacral agenesis is strongly associated with tethered cord syndrome.[3]

Segmental spinal dysgenesis (SSD) may present as dysgenesis or agenesis of a segment of the lumbar, thoracolumbar, or lumbosacral spine, and may include the underlying spinal cord or nerve roots. As such, the prognosis depends on the level and severity of the malformation.[9] The embryological basis for this condition is believed to be defective notochord development, prompting some to speculate SSD may be part of the same spectrum of malformation as sacral agenesis.[4] In the most severe cases, the spinal cord at the level of the abnormality is absent, and one or more vertebrae are absent, effectively bisecting the bony spine and spinal cord. Infants with this degree of abnormality are paraplegic at birth. In less severe cases, there is focal hypoplasia of the spinal cord. Neurological deficit depends on the level and severity of the lesion.[9]

In this study, there were two cases of sacral agenesis, diagnosed at 15w (case 11) and 21w (case 13). Sonographic features included the subjective appearance of a short spine with ossification centres which failed to taper toward each other distally (Figure 20a, Figure 21a). These findings were confirmed at post mortem. Both cases had additional abnormalities detected by ultrasound. Case 11 also presented with a gastroschisis and upper and lower limb arthrogryposis. Case 13 had multiple hemivertebrae and rib abnormalities. Case 13 was the only case in this study that underwent prenatal MRI at 22w. There have been several reports in the literature of the value of prenatal MRI.[7,9,25,27] Unfortunately, MRI images in this case (at 22 weeks) were considered non-diagnostic.

Nomograms for spine length have been developed by De Basio, *et al.*[30] in the first trimester, and Ulm, *et al.* between 14 and 24 weeks of gestation.[31] These authors contend spine length measurements may be a valuable tool to aid diagnosis when skeletal malformations are suspected.

There were no cases of other complex spinal defects in this study, namely dorsal enteric fistula, neurenteric cyst, diastematomyelia and segmental spinal dysgenesis. There have been published reports of prenatal diagnosis of diastematomyelia.[32,33,34] Sonographic features described in these reports include widening of the spinal canal in the coronal plane and an echogenic spur traversing the spinal canal in the transverse plane. There are also reports of prenatal diagnosis of segmental spinal dysgenesis.[23,35,36] Typical sonographic features described include abnormal spine curvature, multiple vertebral segmentation defects and asymmetric ribs. Dorsal enteric fistulas and neurenteric cysts are rare entities. It may be possible to detect a neurenteric cyst with prenatal ultrasound as an anechoic structure in the thorax, anterior to a defect in the vertebral body.

The spectrum of vertebral anomalies in this study shows prenatal ultrasound to be sensitive in the detection of disruptions to the normal sonographic appearance of the fetal spine. The diagnoses for cases in this study (other than open NTD) were often difficult to make at the time. Retrospective analysis of ultrasound images revealed good correlation with post mortem or postnatal imaging, and allowed for development of skills in manipulating 3D datasets. Considering the features of abnormal spine curvature, flared or divergent vertebral arch ossification centres, and the appearance of a short spine, a spectrum of congenital spine anomalies may be grouped according to these sonographic features (Figure 22).

Conclusion

Recognition of a fetal spine abnormality begins with the detection of disruption to the normal appearances of the fetal spine. These can be simply described as flared vertebral arches, abnormal spine curvature, and short spine length. Using these markers it is possible to target the ultrasound examination to seek additional features to aid in the diagnosis of the congenital spine anomaly.

Overall numbers in this study were small; however, the spectrum of abnormalities detected was consistent with reports in the literature and the rarity of these lesions (12 case reports are listed in Appendix 2). It is hoped this framework could form the basis for a future systematic review. In this study cases other than open NTD had a poor prognosis. This invites speculation that perhaps prenatally diagnosed vertebral defects are at the more severe end of the spectrum.

Future works implementing measurements of overall spine length in cases of vertebral abnormalities would aid in the diagnosis of conditions such as sacral agenesis and segmental spinal dysplasia.

Acknowledgements

This study is a condensed version of the main author's research project for the award of Master in Applied Science (Medical Sonography) RMIT University, supported by an ACT Health scholarship for further education of Allied Health Professionals. The author would also like to acknowledge the support of colleagues in the Fetal Medicine Unit, and staff in the departments of Medical Imaging, Pathology and Medical Records.

References

1 Abeywardana S, Sullivan EA 2008. Neural tube defects in Australia. An epidemiological report. Cat.no.PER 45. Sydney: AIHW National Perinatal Statistic Unit.

2 Botto L, Moore C, Khoury M, Erickson D. Neural Tube Defects [Electronic version]. *Medical Progress* 1999; 341 (20): 1509–19.

3 Ross M, Brewer K, Wright V, Agur A. Closed Neural Tube Defects: Neurologic, Orthopedic, and Gait Outcomes. *Pediatric Physical Therapy* 2007; 19: 288–95

4 Tortori-Donato P, Fondelli M, Rossi A, RaybaudC, Cama A, Capra V. Segmental Spinal Dysgenesis: Neuroradiologic Findings with Clinical and Embryological Correlation. *American Journal of Neuroradiology*, 1999; 20: 445–56.

5 Tortori-Donati P, Rossi A, Cama A. Spinal Dysraphism: a review of neuroradiological features with embryological correlation and proposal for a new classification. *Neuroradiology* 2000; 42: 471–91.

6 Rossi A, Gandolfo C, Morana G, Piatelli G, Ravegnani M, Consales

A, Pavanello M, Cama A, Tortori-Donati P. Current Classification and Imaging of Congenital Spinal Abnormalities. *Seminars in Roentgenology* 2006; 41 (4): 250–73.
7 Grimme J, Castillo M. Congenital Anomalies of the Spine [Electronic version]. *Neuroimaging Clinics of North America* 2007; 17: 1–16.
8 Muthukumar, N. Congenital spinal lipomatous malformations Part 1 – classification. *ActaNeurochirurgica*, 2009; 151: 179–88.
9 Tortori-Donati, P, Rossi A, Biancheri R, Cama A. Congenital Malformations of the Spine and Spinal Cord. In: Pediatric Neurology, Part 2. Springer: Berlin Heidelberg 2005. Retrieved 18 February 2010 from RMIT library database.
10 Kaplan K, Spivak J, Bendo J. Embryology of the spine and associated congenital abnormalities [Electronic version]. *The Spine Journal* 2005, 5: 564–576.
11 Sadler TW. Langman's Medical Embryology. 10th ed. Baltimore: Lippincott Williams & Wilkins 2006.
12 Rufener SL, Ibrahin M, Raybaud CA, Parmar HA. Congenital Spine and Spinal Cord Malformations – Pictorial Review. *AJR* 2010; 194: 26–36.
13 ISUOG Guidelines. Sonographic examination of the fetal central nervous system: guidelines for performing the 'basic examination' and the 'fetalneurosonogram'. *Ultrasound Obstet Gynecol* 2007; 29:109–16.
14 Widjaja E, Whitby EH, Paley MNJ, Griffiths PD. Normal fetal lumbar spine on post-mortem MR imaging. *Am J Neuroradiol* 2006; 27: 553–59.
15 Bagnall KM, Harris PF, Jones RM. A radiographic study of the human fetal spine 3. Longitudinal growth. *J Anat* 1979; 128 (4): 777–87.
16 Govender S, Charles RW, Haffejee MR. Level of termination of the spinal cord during normal and abnormal fetal development. *S Afr Med J* 1989; 75: 484–87.
17 Pooh RK, Pooh K. Fetal vertebral structure detected by three-dimensional ultrasound. *Ultrasound Review of Obstetrics and Gynaecology* 2005; 5 (1): 29–33.
18 Budorick NE, Pretorius DH, Grafe MR, Lou KV. Ossification of the fetal spine. *Radiology* 1981; 181: 561–65.
19 Yanagihara T, Hata T. Three-dimensional sonographic visualization of fetal skeleton in the second trimester of pregnancy. *GynecolObstet Invest* 2000; 49: 12–16.
20 Benoit B. The value of three-dimensional ultrasonography in the screening of the fetal skeleton. *Child NervSyst* 2003; 19: 403–9
21 Bulas D. Fetal evaluation of spine dysraphism. *PediatrRadiol* 2010; 40: 1029–37.
22 Debnath UK, Goel V, Harshavardhana N, Webb JK. Congenital scoliosis – Quo Vadis. *Indian J Orthop* 2010; 44 (2): 137–47.
23 Moser J. Evaluation of hemivertebrae and fetal ribs using 3D sonography. *J Diag Med Sonog* 2005; 21 (2): 119–25.
24 Jones KL. Smith's Recognizable Patterns of Human Malformation 6th ed. Philadelphia: Elsevier Saunders; 2006.
25 Simon ER. MRI of the fetal spine. *Pediatr Radiol* 2004; 34: 712–19.
26 Nicolaides K, Campbell S, Gabbe S, Guidetti R. Ultrasound screening for Spina Bifida: cranial and cerebellar signs [Electronic version]. *The Lancet* 1986; 8498: 72–74.
27 Lituania M, Passamonti U. Prenatal Ultrasound: Spine and Spinal cord. In: Pediatric Neurology, Part 2. Springer Berlin Heidelberg 2005.
28 Kim SY, McGahan JP, Boggan JE, McGrew W. Prenatal diagnosis of Lipomyelomeningocele. *J Ultrasound Med* 2000; 19: 801–5.
29 Sohaey R, Oh K, Kennedy A, Ameli J, Selden N. Prenatal diagnosis of tethered spinal cord. *Ultrasound Quarterly* 2009; 25 (2): 83–87.
30 De Basio P, Ginocchio G, Vignolo M, Ravera, G, Venturini PL, Aicardi G. Spine length measurement in the first trimester of pregnancy. *Prenat Diagn* 2002; 22: 818–22.
31 Ulm MR, Kratochwil A, Oberhuemer U, Ulm B, Blaicher W, Bernaschek G. Ultrasound evaluation of fetal spine length between 14 and 24 weeks of gestation. *Prenat Diagn* 1999; 19: 637–41.
32 Fauchon D, Benzie RJ. Diastematomyelia – a case review. *ASUM Ultrasound Bulletin* 2005; 8 (2): 40–41.
33 Has R, Yuksel A, Buyukkurt S, Kalelioglu I, Tatli B. Prenatal diagnosis of diastematomyelia; presentation of eight cases and review of the literature. *Ultrasound ObstetGynecol* 2007; 30: 845–49.
34 Anderson NG, Jordan S, MacFarlane MR, Lovell-Smith M. Diastematomyelia: diagnosis by prenatal sonography. *AJR* 1994; 163: 911–14.
35 Sallout BI, D'Agostini D, Pretorius DH. Prenatal diagnosis of spondylocostaldysostosis with 3-dimensional ultrasonography. *J Ultrasound med* 2006; 25: 539–43.
36 Alvarez de la Rosa M, Padilla Perez AI, de la Torre Fernandez de Vega FJ, TroyanoLuque JM. Genetic counselling in a case of congenital hemivertebrae. *Arch GynecolObstet*2009; 280: 653–58.
37 Bashiri A, Sheizaf B, Burstein E, Landau D, Hershkovitz R, Mazor M. Three dimensional ultrasound diagnosis of caudal regression syndrome at 14 gestational weeks. *Arch Gynecol Obstet* 2009; 280: 505–7.
38 Baxi L, Warren W, Collins M, Timor-Tritsch IE. Early detection of caudal regression syndrome with transvaginal scanning. *Obstet Gynecol* 1990; 75 (3): 486–89.
39 Aslan H, Yanik H, Celikaslan N, Yildrim G, Ceylan Y. Prenatal diagnosis of caudal regression syndrome: a case report. *BMC Pregnancy and Childbirth* 2001; 1. Available at 8http://www.biomedcentral.com/1471–2393/1/8.
40 Chreston J, Sherman SJ. Sonographic detection of Lipomyelomeningocele: A retrospective documentation. *J Clin Ultrasound* 1997; 25: 50–1.
41 Sharoney R, Aviram R, Tohar M, Regev R, Cohen I, Beyth Y, Tepper R. Prenatal sonographic detection of a lipomeningocele as a sacral lesion. *J Clin Ultrasound* 2000; 28: 150–52.

Appendix 1: syndromes associated with vertebral defects

From Smith's Recognisable Patterns of Human Malformation (24)

Frequent feature in:	Occasional feature in:
Alagille syndrome	Aarskog syndrome
Atelosteogenesis type 1	Aase syndrome
Caudal dysplasia sequence	Albright hereditary Osteodystrophy
Cervico-Oculo-Acoustic syndrome	Apert
Distichiasis-Lymphedema syndrome	Baller-Gerold syndrome
Escobar syndrome	Catel-Manke syndrome
Extrophy of cloaca sequence	CHARGE syndrome
Femoral hypoplasia-unusual facies syndrome	Coffin-Siris syndrome
Freeman-Sheldon syndrome	Deletion 5p syndrome
Frontometaphyseal dysplasia	Deletion 9p syndrome
Iniencephaly sequence	Deletion 13q syndrome
Jarcho-Levin syndrome	Deletion 22q11.2 syndrome
Kabuki Syndrome	Down syndrome (T21)
Klippel-Feil sequence	Duplication 3q syndrome
Langer-Giedion syndrome	Duplication 10q syndrome
Lethal multiple pterygium syndrome	Fanconi Pancytopenia syndrome
Metatropic dysplasia	Fetal alcohol syndrome
Multiple synostosis syndrome	Fetal warfarin syndrome
MURCS association	45X syndrome
Noonan syndrome	Freeman-Sheldon syndrome
Occult spinal dysraphism sequence	Gorlin syndrome
Oculo-Auriculo-Vertebral spectrum (Goldenhar syndrome)	Hallermann-Streiff syndrome
Oto-palato-Digital syndrome type 1	Holt-Oram syndrome
Pallister-Hall syndrome	IncontinentiaPigmenti syndrome
Robinow syndrome	Larsen syndrome
Shprintzen-Goldberg syndrome	Marden-Walker syndrome
Simpson-Golabi-Behmel syndrome	Marfan syndrome
Sirenomelia sequence	Marshall-Smith syndrome
Spondylocarpotarsalsynostosis	Microphthalmia-Linear skin defects syndrome
Smith-Magenis syndrome	Miller syndrome
Trisomy 8 syndrome	Monozygotic twinning
VATERR association	Nager syndrome
	Nail-Patella syndrome
	Neurofibromatosis syndrome
	Poland sequence
	Popliteal pterygium syndrome
	Radial aplasia-thrombocytopenia syndrome
	Rubenstein-Taybi syndrome
	Saethre-Chotzen syndrome
	3C syndrome
	Toriello-Carey syndrome
	Trisomy 18 syndrome
	Waardenburg syndrome
	X-linked α-Thallasemia/ mental retardation syndrome

Appendix 2: Review of reported cases of vertebral segmentation and formation abnormalities and closed NTD

Reference	Anomaly	Sonographic features
Sallout, *et al*.[35]	SpondylocostalDysostosis	Abnormal spine curvature (sagittal 2D imaging) Segmental vertebral defects & asymmetric rib spacing (3D imaging)
Alvarez de la Rosa, *et al*.[34]	SpondylothoracicDyostosis	Abnormal spine curvature (sagittal 2D imaging) Thoracic hemivertebrae and rib fusion (3D imaging)
Moser[23]	Jarcho-Levin syndrome	Abnormal spine curvature (sagittal 2D imaging) Multiple hemivertebrae, reduced and asymmetric rib number (3D imaging)
Sohaey, *et al*.[29]	Myelocystocele	Cystic mass within spinal canal (coronal 2D imaging)
Bashiri, *et al*.[37]	Sacral agenesis	Shorter than expected crown-rump length Absent lumbar and sacral vertebrae (2D and 3D imaging) Fixed lower limbs
Baxi, *et al*.[38]	Sacral agenesis	Shorter than expected crown-rump length Termination of spine at lumbar level with flaring of vertebrae (2D imaging) Fixed lower limbs
Aslan, *et al*.[39]	Sacral agenesis	Termination of spine at lumbar level (2D imaging) Fixed lower limbs
Chrestonet, *et al*.[40]	Lipomyelomeningocele	Echogenic areas within spinal canal (coronal 2D imaging)
Sharoney, *et al*.[41]	Lipomeningocele	Semisolid echogenic lumbosacral mass with underlying defects in the lateral aspect of sacral vertebral bodies (2D imaging)
Kim, *et al*.[28]	Lipomyelomeningocele with intradurallipoma	Circumscribed slightly echogenic subcutaneous lumbosacral mass Echogenic mass within spinal canal and low lying spinal cord (2D imaging)
Fauchon & Benzie[32]	Diastematomyelia	Flaring of vertebrae with a central bony spur (transverse & coronal 2D and 3D imaging)
Has, *et al*.[33]	diastematomyelia	Widening of the spinal canal in coronal plane and an echogenic spur traversing the spinal canal in transverse plane (2D imaging)